

# **Revised treatment of wet scavenging processes dramatically improves GEOS-Chem 12.0.0 simulations of surface nitric acid, nitrate, and ammonium over the United States**

Gan Luo, Fangqun Yu, and James Schwab

Atmospheric Sciences Research Center, University at Albany

## **Abstract**

The widely used community model GEOS-Chem 12.0.0 and previous versions have been recognized to significantly overestimate the concentrations of gaseous nitric acid, aerosol nitrate, and aerosol ammonium over the United States. The concentrations of nitric acid are also significantly over-predicted in most global models participating a recent model inter-comparison study. In this study, we show that most or all of this overestimation issue appears to be associated with wet scavenging processes. Replacement of constant in-cloud condensation water (ICCW) assumed in GEOS-Chem standard versions with one varying with location and time from the assimilated meteorology significantly reduces mass loadings of nitrate and ammonium during the wintertime, while the employment of an empirical washout rate for nitric acid significantly decreases mass concentrations of nitric acid and ammonium during the summertime. Compared to the standard version, GEOS-Chem with updated ICCW and washout rate significantly reduces the simulated annual mean mass concentrations of nitric acid, nitrate, and ammonium at surface monitoring network sites in US, from 2.04 to 1.03  $\mu\text{g m}^{-3}$ , 1.89 to 0.88  $\mu\text{g m}^{-3}$ , 1.09 to 0.68  $\mu\text{g m}^{-3}$ , respectively, in much better agreement with corresponding observed values of 0.83, 0.70, and 0.60  $\mu\text{g m}^{-3}$ , respectively. In addition, the agreement of model simulated seasonal variations of corresponding species with measurements is also improved. The updated wet scavenging scheme improves the skill of the model in predicting nitric acid, nitrate, and ammonium

- 1 concentrations which are important species for air quality and climate.

## 1. Introduction

Nitrate and ammonium are important secondary inorganic aerosols in the atmosphere, contributing significantly to total aerosol mass over most polluted regions (Bian et al., 2017) and to aerosol direct radiative forcing over urban and agriculture regions (Bauer et al., 2007; Myhre et al., 2013). The amount of nitrate and ammonium also regulates the concentration of gaseous ammonia which often plays an important role in the formation of new particles (Kirkby et al., 2011; Yu et al., 2018). In addition, nitrate and ammonium help newly formed particles grow to larger sizes suitable for cloud condensation nuclei (Yu and Luo, 2009) and thus can impact aerosol indirect radiative forcing (Twomey, 1977).

Nitric acid, nitrate, and ammonium concentrations are often overestimated by atmospheric models (Pye et al., 2009; Walker et al., 2012; Bian et al., 2017; Zakoura and Pandis, 2018), including the widely used community model GEOS-Chem (e.g., Zhang et al., 2012; Heald et al., 2012). Zhang et al. (2012) studied nitrogen deposition over the US with GEOS-Chem and found both nitric acid and nitrate concentrations are overestimated, especially in wintertime. They suggested that this is the result of excessive nitric acid formation via night time chemistry of heterogeneous  $\text{N}_2\text{O}_5$  hydrolysis. However, Heald et al. (2012) found the overestimate of heterogeneous  $\text{N}_2\text{O}_5$  hydrolysis does not fully account for the nitrate bias and suggested the positive nitrate bias is likely linked with an overestimate of nitric acid concentrations. Heald et al. (2012) investigated other possible causes for the overestimation of nitric acid concentrations arising from uncertainties in daytime formation and dry deposition, and concluded that none of these uncertainties could fully account for the reduction in nitric acid required to correct the nitrate bias. Based on comparisons of simulated nitrate and ammonium aerosol from nine AEROCOM models with ground station and aircraft measurements, Bian et al. (2017) concluded that most models overestimate surface nitric acid volume mixing ratio by a factor of up to 3.9 over North America and the overestimation cannot be simply attributed

1 to model uncertainties. Backes et al. (2016) suggested that uncertainties in the temporal  
2 profiles of ammonia emissions could also contribute significantly to the bias of nitrate  
3 concentrations. However, the impact of ammonia mostly happened during summer time.  
4 Zakoura and Pandis (2018) found significant decrease in nitrate concentration when they  
5 enhanced their model resolution from  $36 \text{ km} \times 36 \text{ km}$  to  $4 \text{ km} \times 4 \text{ km}$  in the PMCAMx  
6 model. However, similar results are not found in global models with much coarser grids  
7 than regional models. All these studies indicate that the overestimation of nitric acid,  
8 nitrate, and ammonium mass concentrations in current atmospheric chemistry models  
9 remains to be resolved.

10 In this study, we proposed an improved treatment of wet scavenging in GEOS-Chem  
11 by considering cloud condensation water variability and empirical washout rate, which  
12 together significantly improve the estimates of nitric acid, nitrate, and ammonium over  
13 the US. GEOS-Chem is a global 3-D model of atmospheric chemistry driven by  
14 meteorological input from the Goddard Earth Observing System (GEOS) of the NASA  
15 Global Modeling and Assimilation Office and includes state-of-the-art routines to deal  
16 with emissions, transport, and other key chemical and physical processes for atmospheric  
17 trace gases and aerosols (Keller et al., 2014; Fontoukis and Nenes, 2007; Martin et al.,  
18 2003; Bey et al., 2001). The improved wet scavenging in GEOS-Chem is described in  
19 section 2. The comparison of model results with surface observations and the changes of  
20 the three species over the US are presented in section 3. Section 4 is the summary and  
21 discussion.

## 22 23 **2. Improved scheme for wet scavenging**

24 Wet scavenging is the main removal pathway for many atmospheric air pollutants.  
25 Two mechanisms are involved in wet scavenging: rainout (in-cloud scavenging) and  
26 washout (below-cloud scavenging). GEOS-Chem treats wet scavenging associated with  
27 stratiform and convective precipitation separately. The wet deposition scheme in

GEOS-Chem is described by Jacob et al. (2000) and Liu et al. (2001) for water-soluble aerosols, and by Amos et al. (2012) for gases. Scavenging of aerosol by snow and cold/mixed precipitation is described by Wang et al. (2011, 2014). The first-order rainout parameterization is based on Giorgi and Chameides (1986).

## 2.1 Impact of in cloud condensed water (ICCW)

For stratiform precipitation, in the most recently released GEOS-Chem version 12.0.0 (GC12), rainout water soluble species is parameterized according to Jacob et al. (2000) and Liu et al. (2001) as

$$F = \frac{P_r}{k \cdot ICCW} (1 - e^{-k \cdot \Delta t}) \quad (1)$$

where  $F$  is the fraction of a water soluble tracer in the grid-box scavenged by rainout,  $\Delta t$  (s) is the model integration time step.  $k$  ( $s^{-1}$ ) is the first-order rainout loss rate (Giorgi and Chameides, 1986) which represents the conversion of cloud water to precipitation water.  $ICCW$  ( $g\ m^{-3}$ ) represents the condensed water content (liquid) within the precipitating cloud (i.e., in cloud) and  $P_r$  ( $g\ m^{-3}\ s^{-1}$ ) is the rate of new precipitation formation (rain only) in the corresponding grid-box.

The rainout loss rate ( $k$ ) represents how fast cloud condensation water can be removed from the atmosphere and thus is critical for rainout scavenging.  $k$  is defined in Jacob et al. (2000) and coded in GC12 (called  $k_{GC12}$  thereafter) as

$$k_{GC12} = k_{min} + \frac{P_r}{ICCW} \quad (2)$$

where  $k_{min}$  ( $s^{-1}$ ) is the minimum value of rainout loss rate derived from the stochastic collection equation which indicates that in one hour at least  $\sim 0.36$  of cloud droplets are lost to autoconversion/accretion (Beheng and Doms 1986). In GC12,  $k_{min}$  is set to be  $0.36\ hr^{-1} = 1 \times 10^{-4}\ s^{-1}$ .

It should be noted that  $P_r$  in Eq. (2) is a grid-box mean value, while  $ICCW$  is an in cloud value. To be physically consistent, we suggest a new expression of  $k$  ( $k_{new}$ ) that replaces grid-box mean  $P_r$  with the corresponding in cloud value  $P_r/f_c$ .

$$k_{new} = k_{min} + \frac{P_r}{f_c \cdot ICCW} \quad (3)$$

where  $f_c$  is the grid-box mean cloud fraction. As we will show later, Eq. (3) gives  $k$  values in much better agreement with those derived from cloud model simulations and observations.

To calculate  $F$ , GC12 uses  $P_r$  from the Modern-Era Retrospective analysis for Research and Applications Version 2 (MERRA2) meteorological fields. For  $ICCW$  in Eqs. 1-3, Jacob et al. (2000) used a constant value of  $1.5 \text{ g m}^{-3}$  and Wang et al. (2011) changed it to  $1 \text{ g m}^{-3}$ . In GC12, the default value of  $ICCW$  is  $1 \text{ g m}^{-3}$ . However,  $ICCW$  in the atmosphere varies with time and location. Here we suggest to use time and location dependent  $ICCW$  (named  $ICCW_t$ ) which can be derived from MERRA2 meteorological fields as

$$ICCW_t = \frac{CW + P_r \cdot \Delta t}{f_c} \quad (4)$$

where  $CW$  is grid-box mean cloud water content, while  $P_r \cdot \Delta t$  represents rain water content produced during the time step  $\Delta t$ . In a previous study, Croft et al. (2016) used cloud liquid and ice water content to replace the fixed  $ICCW$ . However, as shown in Equation 6 in MERRA2's file specification (Bosilovich et al., 2016), cloud water is the residual condensation water after precipitation and is low when precipitation is occurring. Because the fraction of soluble species rained out should equal to the fraction of total condensed water (or  $ICCW$  in our case) converted to rain water, we think that  $ICCW$  in Eq (3) should include rain water (i.e., Eq 4).

Figure 1a shows seasonal variations of  $ICCW_t$  (Eq. 4) averaged throughout the lower troposphere (0–3 km) of the whole globe ( $ICCW_{t\_G}$ ), over all land surface ( $ICCW_{t\_L}$ ), over the oceans ( $ICCW_{t\_O}$ ), and over the continental US ( $ICCW_{t\_US}$ ). For comparisons, the constant values of  $ICCW$  assumed in Jacob et al. (2000) ( $ICCW_{J2000}$ ) and GC12 ( $ICCW_{GC12}$ ) are also shown. The monthly mean values of  $ICCW_{t\_G}$ ,  $ICCW_{t\_L}$ ,  $ICCW_{t\_O}$ ,

1 and  $ICCW_{t\_US}$  vary within the ranges of 0.90–1.03 g m<sup>-3</sup>, 0.30–0.45 g m<sup>-3</sup>, 1.15–1.26 g  
 2 m<sup>-3</sup>, and 0.21–0.53 g m<sup>-3</sup>, respectively. This figure shows that  $ICCW_{t\_G}$  is close to the  
 3 assumed  $ICCW$  value of 1 g m<sup>-3</sup> used in GC12. As can be seen from Fig.1a,  $ICCW_{t\_O}$  is  
 4 greater than 1 g m<sup>-3</sup>, but  $ICCW_{t\_L}$  is much less than the constant value of 1 g m<sup>-3</sup> assumed  
 5 in GC12. The mean  $ICCW$  over the continental US (bright green line) is close to  $ICCW_{t\_L}$   
 6 (olive line), and is ~ 5 times less than the assumed value in GC12 during the wintertime  
 7 and ~ 2 times less during the summertime. As we will show later, the constant  $ICCW$  of 1  
 8 g m<sup>-3</sup> assumed in GC12 leads to significant underestimation of rainout over the  
 9 continental US, especially during the wintertime.

10 Figure 1b shows seasonal variations of mean  $k_{GC12}$ ,  $k_{new}$ , and  $k_{new\_ICCW_t}$  in the lower  
 11 troposphere (0-3 km) of the continental US. Referring to Eq. (2), the figure shows that  
 12  $k_{GC12}$  is dominated by  $k_{min}$  (which is physically unsound) and thus shows negligible  
 13 seasonal variation. Conversely,  $k_{new}$  is low in the wintertime and high in the  
 14 summertime.  $k_{new\_ICCW_t}$  is 2.3 times higher than  $k_{new}$  during January and 1.6 times higher  
 15 than  $k_{new}$  during July. Both  $k_{new}$  and  $k_{new\_ICCW_t}$  are within the range of rainout loss rates  
 16 (10<sup>-4</sup>–10<sup>-3</sup> s<sup>-1</sup>) indicated by cloud model simulations and estimates based on observations  
 17 (Giorgi and Chameides, 1986).

18 From Eqs. (1), (3), and (4), we can get the updated parameterization for rainout loss  
 19 fraction at each location and time step

$$20 \quad F = \frac{f_c \cdot P_r}{k_{new\_ICCW_t} (CW + P_r \cdot \Delta t)} \left( 1 - e^{-E_r \cdot k_{new\_ICCW_t} \cdot \Delta t} \right) \quad (5)$$

21

## 22 **2.2 Impact of empirical washout rate on nitric acid wet scavenging**

23 Still considering the case of stratiform precipitation in GOES-Chem, the fraction of  
 24 aerosols and HNO<sub>3</sub> within a grid-box that is scavenged by washout over a time step is  
 25 parameterized as (Wang et al., 2011; Liu et al., 2001; Jacob et al., 2000)

$$1 \quad F_{wash} = f_r(1 - \exp(-k_{wash}\Delta t)) \quad (6)$$

$$2 \quad f_r = \max\left(\frac{P_r}{k \cdot ICCW}, f_{top}\right) \quad (7)$$

$$3 \quad k_{wash} = \Lambda \left(\frac{P_r}{f_r}\right)^b \quad (8)$$

4 where  $f_r$  is the horizontal areal fraction of the grid-box experiencing precipitation and  $f_{top}$   
5 is the value of  $f_r$  in the layer overhead ( $f_{top} = 0$  at the top of the precipitating column).  
6  $k_{wash}$  is washout rate,  $\Lambda$  is washout scavenging coefficient, and  $b$  is an exponential  
7 coefficient. In the original GEOS-Chem,  $\Lambda = 1 \text{ cm}^{-1}$  and  $b = 1$  for both aerosols and nitric  
8 acid (Liu et al., 2001; Jacob et al., 2000).

9 It has been well recognized that, for aerosols,  $\Lambda$  and  $b$  depend on particle size (Wang  
10 et al., 2010; Feng, 2007; Andronache et al., 2006; Henzing et al., 2006; Laakso et al.,  
11 2003). Feng (2007) suggested values of  $b = 0.62$ ,  $0.61$ , and  $0.8$  for particles in nucleation  
12 (diameter  $1 \text{ nm} - 40 \text{ nm}$ ), accumulation ( $40 \text{ nm} - 2.5 \text{ }\mu\text{m}$ ), and coarse mode ( $>2.5 \text{ }\mu\text{m}$ ),  
13 respectively. Many studies indicate that there are large difference between existing  
14 theoretical and observed size-resolved washout rates (Wang et al., 2010; Andronache et  
15 al., 2006; Henzing et al., 2006; Laakso et al., 2003). For particles within the diameter  
16 range of  $0.01 - 2 \text{ }\mu\text{m}$ , size-resolved washout rates derived from analytical formulas are one  
17 to two orders of magnitude smaller than those derived from field measurements (e.g.,  
18 Wang et al., 2010). This large difference could result from turbulent flow fluctuations  
19 (Andronache et al. 2006; Khain and Pinsky, 1997), vertical diffusion process (Zhang et al.,  
20 2004), and droplet-particle collection mechanisms (Park et al., 2005).

21 In GC12,  $\Lambda$  and  $b$  for aerosols are parameterized as a function of particle size modes  
22 (Wang et al., 2011), following Feng (2007). For nitric acid, GC12 keeps  $\Lambda = 1 \text{ cm}^{-1}$  and  $b$   
23  $= 1$ , unchanged from the original GEOS-Chem parameters. In this study, we employ the  
24 size-dependent aerosol washout parameterization derived from six years of field  
25 measurements over forests in southern Finland (Laakso et al., 2003; Wang et al., 2010).  
26 We further estimate nitric acid washout scavenging coefficients by referring to field



1 measurements for particles of 10 nm (Laakso et al., 2003) and the theoretical dependence  
 2 of scavenging coefficients on particle sizes for particles  $< 10$  nm (Henzing et al., 2006).  
 3 The collection efficiency of particles smaller than 10 nm by rain droplets is dominated by  
 4 Brownian diffusion, and in this regard we can treat nitric acid as a single molecule (or  
 5 particle) with diameter of 0.5 nm. Through this approach, we derive empirical  $K_{wash}$  value  
 6 for nitric acid to be  $3 \times 10^{-3} \text{ s}^{-1}$  when rain rate is  $1 \text{ mm h}^{-1}$ . This empirical value is about  
 7 two orders of magnitude larger than the corresponding  $K_{wash}$  value in GC12 ( $0.1 \text{ hr}^{-1} = 2.8$   
 8  $\times 10^{-5} \text{ s}^{-1}$ ). For the dependence of  $K_{wash}$  on rain rate, we adopt the  $b$  value of 0.62 for  
 9 nucleation mode particles (diameter 1 nm – 40 nm) (Feng, 2007) for nitric acid. With this  
 10 empirical  $b$  value of 0.62 and empirical  $K_{wash}$  of  $3 \times 10^{-3} \text{ s}^{-1}$ , we derive an empirical  $\Lambda$   
 11 value for nitric acid of 2. It should be noted that the unit of empirical  $\Lambda$  is not  $\text{cm}^{-1}$  when  
 12  $b$  is not unity. In our parameterization (Eq. 8),  $\Lambda=2$  and  $P_r$  should be in the unit of  $\text{cm s}^{-1}$ .  
 13 Washout rates for water soluble aerosols are using the empirical values from Laakso et al.  
 14 (2003), while washout rates for water insoluble aerosols are still using the values from  
 15 Feng (2007). No change is made to washout by snow, which is based on the approach  
 16 described in Wang et al. (2011).

17 For convective precipitation, scavenging in convective updrafts are coupled with  
 18 convective transport (e.g., Liu et al., 2001). Furthermore, MERRA2 meteorological fields  
 19 do not provide convective cloud fraction and cloud water content. Therefore, the updated  
 20 wet scavenging method discussed above for stratiform precipitation cannot be directly  
 21 applied to convective precipitation rainout scavenging in GEOS-Chem. However, the  
 22 empirical values for water soluble aerosol and nitric acid washout are also applied to  
 23 convective washout in the present study as Case 4.

### 24 25 **3. Model simulations and results**

26 To study the impacts of various updates to the wet scavenging as described in  
 27 Section 2 on model simulated nitric acid, nitrate, and ammonium mass concentrations, we

run GEOS-Chem for 4 cases: (1) standard GC12 parameterizations for rainout and washout, called GC12; (2) same as the Case GC12 except  $k_{new}$  in Eq. 3 is used, called Knew; (3) same as the Case Knew except  $ICCW_t$  from MERRA2 (Eq. 4) is used, called  $ICCW_t$ ; (4) same as the Case  $ICCW_t$  except empirical washout rates for nitric acid and water soluble aerosols are used, called  $ICCW_t\_EW$ . For each case, we carry out simulations from December 2010 to December 2011, with the first month as spin-up. The model horizontal resolution is  $2^\circ \times 2.5^\circ$  and vertically there are 47 layers. The present analysis focuses on the continental United States. We compared simulated nitric acid with in-situ observations at Clean Air Status and Trends Network (CASTNET) sites, simulated nitrate and ammonium with in-situ observations at Interagency Monitoring of Protected Visual Environments (IMPROVE) and Chemical Speciation Network (CSN) sites. For 2011, there were 74 sites with available nitric acid observations from CASTNET. For the same year, IMPROVE had 120 sites with available nitrate and ammonium observations, while CSN had 94 sites with available nitrate observations and 63 sites with available ammonium observations.

The effects of different modifications to the GC12 wet scavenging parameterization on model simulated nitric acid, nitrate, and ammonium mass concentrations are shown in Figures 2-3 and Table 1. Most of the changes of mass concentrations of the 3 species over the US are caused by the changes of cloud condensation variability and/or empirical washout rate. The impact of new rainout loss rate ( $k_{new}$ ) is relatively small because of the cancelling effect of  $k$  in the denominator and also in the exponent in Eq. 1. As shown in Figs. 2a-2b and Table 1, all cases except  $ICCW_t\_EW$  overestimate nitric acid at CASTNET sites by a factor 2–3 in both wintertime and summertime. Consideration of cloud condensation water variability slightly reduces nitric acid in January and December but has negligible effect during other months. The inclusion of the empirical washout rate reduces the normalized mean bias (NMB) of nitric acid from 125 % to 24 % (Table 1). Figures 2c and 2d show the impacts of improved wet scavenging on nitrate. It is clear that

GC12 significantly overestimates nitrate concentration at most sites especially during the wintertime, in agreement with previous studies (Heald et al., 2012; Walker et al., 2012). Replacing constant ICCW with variable  $ICCW_t$  reduces the NMB of nitrate from 170 % to 84 %. ICCW has significant impact on reducing nitrate mass concentration during the wintertime and a smaller impact during the summertime. Wintertime bias of nitrate was reduced from  $2 \mu\text{g m}^{-3}$  to  $0.7 \mu\text{g m}^{-3}$ . The change of washout rate from theoretical value to empirical formula results in an additional 59 % reduction of NMB for nitrate and impacts nitrate mass concentration significantly both in the winter and in the summer. For ammonium, NMB is reduced from 85 % to 43 % after considering rainout with variable cloud condensation water. Similar to nitrate, the impact of ICCW is large during the wintertime and smaller during the summer time. After considering empirical washout, the NMB of ammonium is reduced to 13 %. While the update in the wet scavenging parameterization significantly improves agreement of the model simulated mass concentrations of nitric acid, nitrate, and ammonium over the US with those observed, it does not affect the correlation coefficients of annual mean values (Table 1) which are dominated by spatial distributions (Fig. 3).

Figure 3 shows the horizontal distributions of surface layer nitric acid, nitrate, and ammonium mass concentrations over the US for case GC12 (a-c) and case  $ICCW_t\_EW$  (d-f). For comparison, annual mean mass concentrations observed at CASTNET, IMPROVE, and CSN sites are shown in filled cycles. The spatial pattern of the simulated concentrations of the three species for the  $ICCW\_EW$  case is close to those for the GC12 case. High concentrations of nitric acid are mainly located at northeastern, southern, and western US with the values up to  $2\text{--}4 \mu\text{g m}^{-3}$  based on GC12 (Fig. 3a) and  $1\text{--}2 \mu\text{g m}^{-3}$  based on  $ICCW_t\_EW$  (Fig. 3d). Horizontal distribution of nitrate is different from that of nitric acid. Nitrate is mainly located at the Ohio valley region and the Northeastern US with values up to  $4\text{--}5 \mu\text{g m}^{-3}$  based on GC12 (Fig. 3b) and  $1\text{--}3 \mu\text{g m}^{-3}$  based on  $ICCW_t\_EW$  (Fig. 3e). Ammonium shows a similar horizontal distribution to that of

1 nitrate, but its value is ~50 % lower than nitrate concentration. For the whole continental  
2 US domain, the annual mean nitric acid, nitrate, and ammonium concentration in the  
3 model surface layer are reduced from  $1.48 \mu\text{g m}^{-3}$  to  $0.78 \mu\text{g m}^{-3}$ ,  $1.03 \mu\text{g m}^{-3}$  to  $0.46 \mu\text{g}$   
4  $\text{m}^{-3}$ ,  $0.76 \mu\text{g m}^{-3}$  to  $0.47 \mu\text{g m}^{-3}$ , respectively. The percentage changes for nitric acid,  
5 nitrate, and ammonium concentrations averaged within the domain are -47%, -55%, and  
6 -38%, respectively. The improved wet scavenging treatment had significant impacts on  
7 nitric acid, nitrate, and ammonium modeling over the US. As can be seen from Figs.  
8 3a-3f (and also Fig. 2 and Table 2), simulated nitric acid, nitrate, and ammonium mass  
9 concentrations over the US based on the updated wet scavenging parameterization (i.e.,  
10  $\text{ICCW}_t\text{EW}$ ) are in much better agreement with in-situ measurements.

#### 12 **4. Summary and discussions**

13 We present an improved wet scavenging parameterization for using in GEOS-Chem  
14 by considering cloud condensation water variability and an empirical washout rate. The  
15 updated parameterization significantly reduces the overestimation of simulated annual  
16 mean mass concentrations of nitric acid, nitrate, and ammonium at CASTNET,  
17 IMPROVE, and CSN sites in US, from 2.04 to 1.03 (observation:  $0.83 \mu\text{g m}^{-3}$ ), 1.89 to  
18  $0.88 \mu\text{g m}^{-3}$  (observation:  $0.70 \mu\text{g m}^{-3}$ ), 1.09 to  $0.68 \mu\text{g m}^{-3}$  (observation:  $0.60 \mu\text{g m}^{-3}$ ), respectively. In  
19 addition, the agreement of model simulated seasonal variations of corresponding species  
20 with measurements is also improved. The updated wet scavenging scheme provides a  
21 partial solution to the persistent problem of nitric acid and nitrate overestimation in the  
22 widely used community model GEOS-Chem (e.g., Heald et al., 2012) and thus improve  
23 the skill of the model in predicting nitric acid, nitrate, and ammonium concentrations. It  
24 should be noted that in the present study the cloud condensation water variability is  
25 considered only for stratiform cloud rainout. Convective cloud removal is important  
26 (especially for tropical regions) and is necessary to be studied as well, calling for the  
27 output of convective cloud fraction and cloud water content fields in future GMAO

1 reanalysis products.

2       The empirical washout rate suggested in the present work will also help to resolve  
3 the significant over-prediction of nitric acid by most of the 9 global models participating  
4 in the Aerosol Comparisons between Observations and Models (AeroCom) phase III  
5 study (Bian et al., 2017). Due to large difference in nitric acid washout rate based on  
6 theoretical and field studies and the importance of this rate, further research is needed to  
7 better understand the underlying reasons and reduce the difference. At the time being, we  
8 recommend the empirical values to be used in models. The revised rainout scheme  
9 presented in this study can be applied to other atmospheric chemistry models assuming  
10 constant cloud condensation water. The changes of nitrate and ammonium mass  
11 concentrations not only impact particle growth but also influence ammonia  
12 concentrations which are important for aerosol nucleation (Kirkby et al., 2011; Yu et al.,  
13 2018), via the equilibrium of sulfate-nitrate-ammonium. The updated scheme presented  
14 in this study has potential implications to new particle formation, particle growth, aerosol  
15 size, CCN number concentration and associated radiative forcing, which will be the  
16 subjects of future research.

17       In this study, we only evaluated the impacts of the updated wet scavenging  
18 parameterization on nitric acid, nitrate, and ammonium concentrations at the surface level  
19 over the US. The impacts of the updated wet scavenging parameterization on the  
20 concentrations all major aerosols over the whole globe should be carefully assessed  
21 against relevant measurements in future studies. In addition, the impact of the updated  
22 treatment of wet scavenging on aerosol vertical profile and mass loading shall be  
23 investigated. Previous study by Liu et al. (2001) indicate that Pb-210 is a good tracer for  
24 testing wet deposition in GEOS-Chem. It will be helpful to carry out Pb-210 simulation  
25 to further evaluate the updated wet scavenging parameterization.

26  
27 Code and data availability. The code of GEOS-Chem 12.0.0 is available through the

GEOS-Chem distribution web-page  
[http://wiki.seas.harvard.edu/geos-chem/index.php/GEOS-Chem\\_12](http://wiki.seas.harvard.edu/geos-chem/index.php/GEOS-Chem_12). All measurement data are publicly available.

Author contributions. GL and FY proposed and implemented the revised wet scavenging scheme and validated model simulations with surface observations. JS provided useful suggestions to improve this work. All authors contributed to the writing and editing of the paper.

Competing interests. The authors declare that they have no conflict of interest.

Acknowledgments. This work is supported by NYSERDA under contract 100416, NASA under grant NNX13AK20G, and NSF under grant 1550816. We would like to acknowledge Interagency Monitoring of Protected Visual Environments (IMPROVE), Chemical Speciation Network (CSN), and Clean Air Status and Trends Network (CASTNET) for the in-site measurement data. GEOS-Chem is a community model maintained by the GEOS-Chem Support Team at Harvard University.

## References

- Andronache, C., Grönholm, T., Laakso, L., Phillips, V., and Venäläinen, A., Scavenging of ultrafine particles by rainfall at a boreal site: observations and model estimations, *Atmos. Chem. Phys.*, 6, 4739-4754, <https://doi.org/10.5194/acp-6-4739-2006>, 2006.
- Backes, A., Aulinger, A., Bieser, J., Matthias, V., Quante, M., Ammonia emissions in Europe, part I: development of a dynamical ammonia emission inventory. *Atmos. Environ.* 131, 55–66, 2016.
- Bauer, S. E., Koch, D., Unger, N., Metzger, S. M., Shindell, D. T., and Streets, D. G.: Nitrate aerosols today and in 2030: a global simulation including aerosols and

1 tropospheric ozone, *Atmos. Chem. Phys.*, 7, 5043-5059,  
 2 <https://doi.org/10.5194/acp-7-5043-2007>, 2007.

3 Beheng, K. D. and G. Doms, A general formulation of collection rates of cloud and  
 4 raindrops using the kinetic equation and comparison with parameterizations. *Beitr.*  
 5 *Phys. Atmos.*, 59, 66–84, 1986.

6 Bey, I., D. J. Jacob, R. M. Yantosca, J. A. Logan, B. Field, A. M. Fiore, Q. Li, H. Liu, L. J.  
 7 Mickley, and M. Schultz, Global modeling of tropospheric chemistry with  
 8 assimilated meteorology: Model description and evaluation, *J. Geophys. Res.*, 106,  
 9 23,073 – 23,096, doi:10.1029/2001JD000807, 2001.

10 Bian, H., Chin, M., Hauglustaine, D. A., Schulz, M., Myhre, G., Bauer, S. E., Lund, M. T.,  
 11 Karydis, V. A., Kucsera, T. L., Pan, X., Pozzer, A., Skeie, R. B., Steenrod, S. D.,  
 12 Sudo, K., Tsigaridis, K., Tsimpidi, A. P., and Tsyro, S. G., Investigation of global  
 13 particulate nitrate from the AeroCom phase III experiment, *Atmos. Chem. Phys.*, 17,  
 14 12911-12940, <https://doi.org/10.5194/acp-17-12911-2017>, 2017.

15 Bosilovich, M. G., R. Lucchesi, and M. Suarez: MERRA-2: File Specification. GMAO  
 16 Office Note No. 9 (Version 1.1), 73 pp, available from  
 17 [http://gmao.gsfc.nasa.gov/pubs/office\\_notes](http://gmao.gsfc.nasa.gov/pubs/office_notes), 2016.

18 Croft, B., Martin, R. V., Leaitch, W. R., Tunved, P., Breider, T. J., D’Andrea, S. D., and  
 19 Pierce, J. R.: Processes controlling the annual cycle of Arctic aerosol number and  
 20 size distributions, *Atmos. Chem. Phys.*, 16, 3665-3682,  
 21 <https://doi.org/10.5194/acp-16-3665-2016>, 2016.

22 Feng, J., A 3-mode parameterization of below-cloud scavenging of aerosols for use in  
 23 atmospheric dispersion models, *Atmos. Environ.*, 41, 6808–6822, 2007.

24 Fountoukis, C., and A. Nenes, ISORROPIA II: A computationally efficient  
 25 thermodynamic equilibrium model for  
 26  $K^+-Ca^{2+}-Mg^{2+}-NH_4^+-Na^+-SO_4^{2-}-NO_3^- -Cl-H_2O$  aerosols, *Atmos. Chem. Phys.*,  
 27 7(17), 4639-4659, 2007.

Giorgi, F., and W. L. Chameides, Rainout lifetimes of highly soluble aerosols and gases as inferred from simulations with a general circulation model, *J. Geophys. Res.*, 91(D13), 14367–14376, doi:10.1029/JD091iD13p14367, 1986.

Heald, C. L., Collett Jr., J. L., Lee, T., Benedict, K. B., Schwandner, F. M., Li, Y., Clarisse, L., Hurtmans, D. R., Van Damme, M., Clerbaux, C., Coheur, P.-F., Philip, S., Martin, R. V., and Pye, H. O. T., Atmospheric ammonia and particulate inorganic nitrogen over the United States, *Atmos. Chem. Phys.*, 12, 10295–10312, <https://doi.org/10.5194/acp-12-10295-2012>, 2012.

Henzing, J. S., Olivi'e, D. J. L., and van Velthoven, P. F. J., A parameterization of size resolved below cloud scavenging of aerosol by rain, *Atmos. Chem. Phys.*, 6, 3363–3375, doi:10.5194/acp-6-3363-2006, 2006.

Jacob, D. J., Liu, H., Mari, C., and Yantosca, B. M., Harvard wet deposition scheme for GMI, [acmg.seas.harvard.edu/geos/wiki\\_docs/deposition/wetdep.jacob\\_etal\\_2000.pdf](http://acmg.seas.harvard.edu/geos/wiki_docs/deposition/wetdep.jacob_etal_2000.pdf), 2000.

Keller, C. A., M. S. Long, R. M. Yantosca, A. M. Da Silva, S. Pawson, and D. J. Jacob, HEMCO v1.0: A versatile, ESMF-compliant component for calculating emissions in atmospheric models, *Geosci. Model Devel.*, 7, 1409–1417, 2014.

Khain, A. P. and Pinsky, M. B., Turbulence effects on the collision kernel, II: Increase of the swept volume of colliding drops, *Q. J. Roy. Meteor. Soc.*, 123, 1543–1560, 1997.

Kirkby, J. and co-authors, Role of sulphuric acid, ammonia and galactic cosmic rays in atmospheric aerosol nucleation, *Nature*, 476, 429–433, 2011.

Laakso, L., Grönholm, T., Rannik, U., Kosmale, M., Fiedler, V., Vehkamäki, H., and Kulmala, M., Ultrafine particle scavenging coefficients calculated from 6 years field measurements, *Atmos. Environ.*, 37, 3605–3613, 2003.

Liu, H. Y., Jacob, D. J., Bey, I., and Yantosca, R. M., Constraints from Pb-210 and Be-7 on wet deposition and transport in a global three-dimensional chemical tracer model



1 driven by assimilated meteorological fields, *J. Geophys. Res.-Atmos.*, 106,  
2 12109–12128, 2001.

3 Martin, R. V., Jacob, D. J., Yantosca, R. M., Chin, M., and Ginoux, P., Global and  
4 regional decreases in tropospheric oxidants from photochemical effects of aerosols, *J.*  
5 *Geophys. Res.*, 108, 4097, doi:10.1029/2002JD002622, 2003.

6 Myhre, G., Samset, B. H., Schulz, M., Balkanski, Y., Bauer, S., Berntsen, T. K., Bian, H.,  
7 Bellouin, N., Chin, M., Diehl, T., Easter, R. C., Feichter, J., Ghan, S. J.,  
8 Hauglustaine, D., Iversen, T., Kinne, S., Kirkevåg, A., Lamarque, J.-F., Lin, G., Liu,  
9 X., Lund, M. T., Luo, G., Ma, X., van Noije, T., Penner, J. E., Rasch, P. J., Ruiz, A.,  
10 Seland, Ø., Skeie, R. B., Stier, P., Takemura, T., Tsigaridis, K., Wang, P., Wang, Z.,  
11 Xu, L., Yu, H., Yu, F., Yoon, J.-H., Zhang, K., Zhang, H., and Zhou, C., Radiative  
12 forcing of the direct aerosol effect from AeroCom Phase II simulations, *Atmos.*  
13 *Chem. Phys.*, 13, 1853-1877, <https://doi.org/10.5194/acp-13-1853-2013>, 2013.

14 Park, S. H., Jung, C. H., Jung, K. R., Lee, B. K., and Lee, K. W., Wet scrubbing of  
15 polydisperse aerosols by freely falling droplets, *Aerosol Sci.*, 36, 1444–1458, 2005.

16 Pye, H. O. T., H. Liao, S. Wu, L. J. Mickley, D. J. Jacob, D. K. Henze, and J. H. Seinfeld,  
17 Effect of changes in climate and emissions on future sulfate - nitrate - ammonium  
18 aerosol levels in the United States, *J. Geophys. Res.*, 114, D01205, doi:  
19 10.1029/2008JD010701, 2009.

20 Twomey, S., The influence of pollution on the shortwave albedo of clouds, *J. Atmos. Sci.*,  
21 34, 1149–1152, 1977.

22 Walker, J., M., Philip, S., Martin, R. V., and Seinfeld, J. H., Simulation of nitrate, sulfate,  
23 and ammonium aerosols over the United States, *Atmos. Chem. Phys.*, 12,  
24 11213–11227, <https://doi.org/10.5194/acp-12-11213-2012>, 2012.

25 Wang, Q., D.J. Jacob, J.A. Fisher, J. Mao, E.M. Leibensperger, C.C. Carouge, P. Le Sager,  
26 Y. Kondo, J.L. Jimenez, M.J. Cubison, and S.J. Doherty, Sources of carbonaceous  
27 aerosols and deposited black carbon in the Arctic in winter-spring: implications for

1 radiative forcing, *Atmos. Chem. Phys.*, 11, 12,453-12,473, 2011.

2 Wang, X., Zhang, L., and Moran, M. D., Uncertainty assessment of current size-resolved  
3 parameterizations for below-cloud particle scavenging by rain, *Atmos. Chem. Phys.*,  
4 10, 5685-5705, <https://doi.org/10.5194/acp-10-5685-2010>, 2010.

5 Yu, F., Nadykto, A. B., Herb, J., Luo, G., Nazarenko, K. M., and Uvarova, L. A.,  
6 H<sub>2</sub>SO<sub>4</sub>–H<sub>2</sub>O–NH<sub>3</sub> ternary ion-mediated nucleation (TIMN): kinetic-based model  
7 and comparison with CLOUD measurements, *Atmos. Chem. Phys.*, 18,  
8 17451-17474, <https://doi.org/10.5194/acp-18-17451-2018>, 2018.

9 Yu, F. and Luo, G., Simulation of particle size distribution with a global aerosol model:  
10 contribution of nucleation to aerosol and CCN number concentrations, *Atmos. Chem.*  
11 *Phys.*, 9, 7691-7710, <https://doi.org/10.5194/acp-9-7691-2009>, 2009.

12 Zakoura M. and S.N. Pandis, Overprediction of aerosol nitrate by chemical transport  
13 models: The role of grid resolution. *Atmos. Environ.* 187, 390-400, 2018.

14 Zhang, L., Jacob, D.J., Knipping, E.M., Kumar, N., Munger, J.W., Carouge, C.C., Van  
15 Donkelaar, A., Wang, Y.X., Chen, D., Nitrogen deposition to the United States:  
16 distribution, sources, and processes. *Atmos. Chem. Phys.* 12, 4539–4554, 2012.

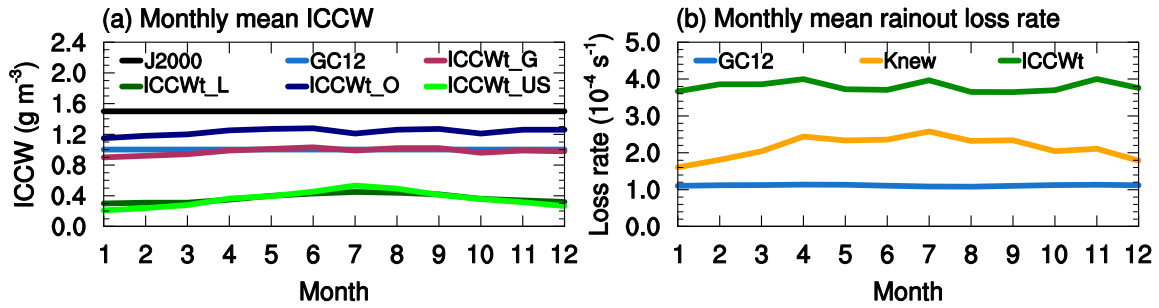
17 Zhang, L., Michelangeli, D. V., and Taylor, P. A., Numerical studies of aerosol  
18 scavenging in low-level, warm stratiform clouds and precipitation, *Atmos. Environ.*,  
19 38, 4653–4665, 2004.

20

1 Table 1. Observed annual mean surface concentrations of  $\text{HNO}_3$ , nitrate, and ammonium  
2 at CASTNET, IMPROVE, and CSN sites. Annual mean surface concentrations (Mean),  
3 normalized mean bias (NMB), and correlation coefficient ( $r$ ) between observed and  
4 simulated annual mean values for the 3 species by GC12, Knew,  $\text{ICCW}_t$ , and  $\text{ICCW}_t\text{EW}$   
5 cases.

|                          | $\text{HNO}_3$                   |            |      | NIT                              |            |      | NH4                              |            |      |
|--------------------------|----------------------------------|------------|------|----------------------------------|------------|------|----------------------------------|------------|------|
|                          | Mean<br>( $\mu\text{g m}^{-3}$ ) | NMB<br>(%) | $r$  | Mean<br>( $\mu\text{g m}^{-3}$ ) | NMB<br>(%) | $r$  | Mean<br>( $\mu\text{g m}^{-3}$ ) | NMB<br>(%) | $r$  |
| Observation              | 0.83                             |            |      | 0.70                             |            |      | 0.60                             |            |      |
| GC12                     | 2.04                             | 145.1      | 0.73 | 1.89                             | 168.1      | 0.53 | 1.09                             | 81.4       | 0.75 |
| Knew                     | 2.05                             | 146.8      | 0.73 | 1.90                             | 170.5      | 0.53 | 1.11                             | 84.5       | 0.75 |
| $\text{ICCW}_t$          | 1.87                             | 125.0      | 0.74 | 1.29                             | 83.5       | 0.57 | 0.86                             | 42.7       | 0.78 |
| $\text{ICCW}_t\text{EW}$ | 1.03                             | 24.2       | 0.72 | 0.88                             | 25.0       | 0.57 | 0.68                             | 12.8       | 0.78 |

6  
7  
8



9

10 Figure 1. (a) Monthly variations of ICCW averaged over the lower troposphere layers of  
11 the whole globe (maroon), global land areas (olive), global oceans (navy), and  
12 continental US (green) from MERRA2, along with constant ICCW values assumed in  
13 J2000 (black) and GC12 (blue). (b) Monthly variations of the rainout loss rate averaged  
14 in the lower troposphere layers of the continental US based on Eq. (2) (i.e, GC12) and Eq.  
15 (3) with constant ICCW of  $1 \text{ g m}^{-3}$ , and Eq. (3) with MERRA2 ICCW (Eq. 4).

16

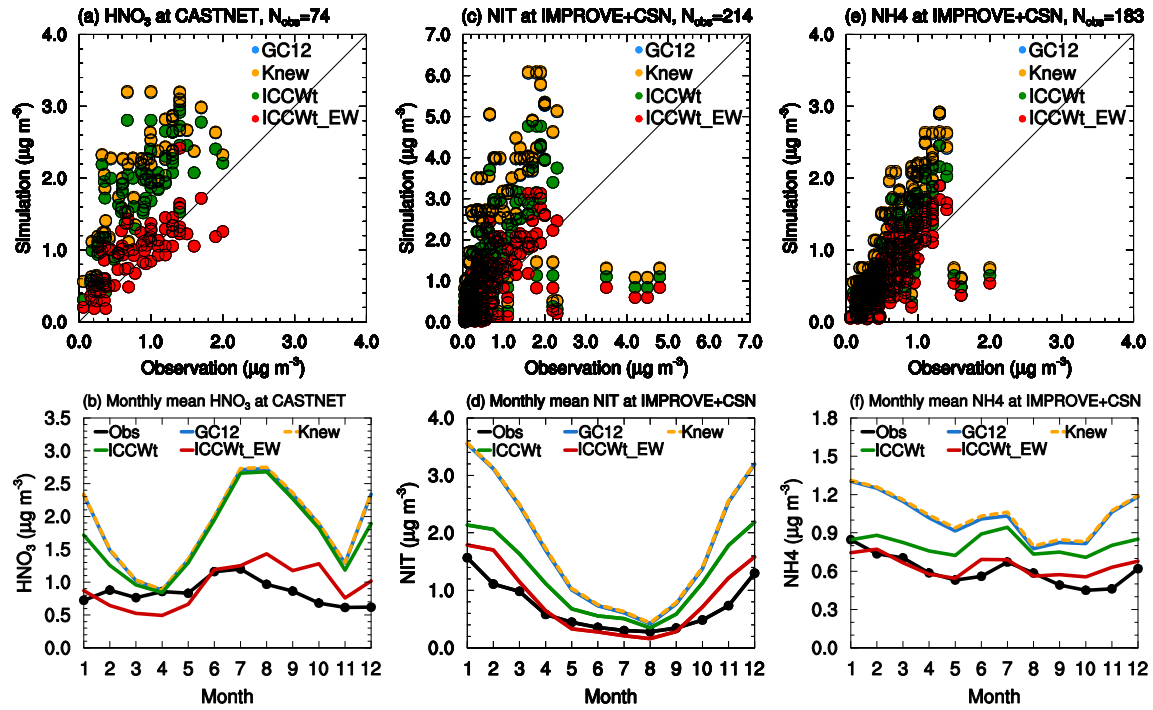


Figure 2. (a) Scatter plot of observed and simulated annual mean  $\text{HNO}_3$  at CASTNET sites and (b) monthly variations of median for year 2011 showing the comparison between nitric acid mass concentrations observed at CASTNET sites (black) and simulated by GC12 (blue), Knew (yellow dash),  $\text{ICCW}_t$  (green), and  $\text{ICCW}_t\text{-EW}$  (red) cases. (c) and (d) are the same as (a) and (b) but for nitrate at IMPROVE+CSN sites. (e) and (f) are the same as (a) and (b) but for ammonium at IMPROVE+CSN sites. It is worthy of note that the differences between G12 (blue) and Knew (yellow dash) are small.

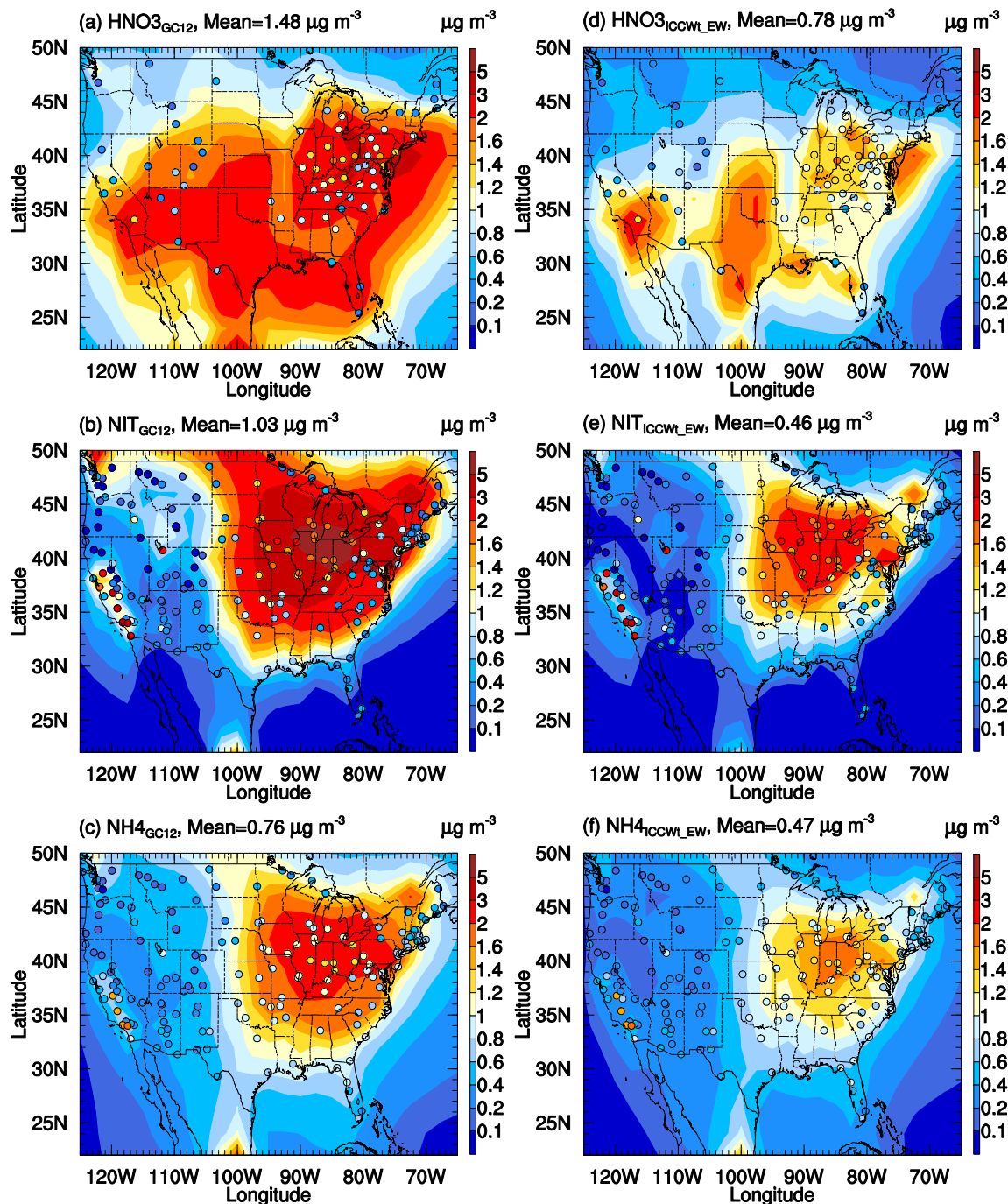


Figure 3. Horizontal distributions of surface layer nitric acid, nitrate, and ammonium simulated by the GC12 case (a-c) and the ICCW<sub>t</sub>\_EW case (d-f). Filled circles are annual mean surface mass concentrations observed at CASTNET, IMPROVE, and CSN for corresponding species.